

Chiral Recognition in Diaziridine Clusters and the Problem of Racemization Waves

Ibon Alkorta* and Jose Elguero

Instituto de Química Médica (C.S.I.C), Juan de la Cierva, 3, 28006-Madrid, Spain

Krzysztof Zborowski

Faculty of Chemistry, Jagiellonian University, 3 Ingardena Street, 30-060 Krakow, Poland

Received: October 25, 2006; In Final Form: November 30, 2006

Theoretical calculations (B3LYP/6-31+G**) of chiral clusters of diaziridines have been carried out. Five configurations of chiral and nonchiral clusters with up to eight monomers have been considered. The proton transfer within the neutral and protonated clusters has been studied as a possible source of racemization waves. The optical rotatory power (ORP) has been calculated for the neutral and protonated homochiral clusters. The results show that the clusters with alternated chiral molecules are the preferred ones and that the proton transfer proceeds with low energetic barriers in the protonated systems. The ORP results are very dependent on the shape of the clusters and the neutral or protonated state of them.

Introduction

The tetrahedral bonding characteristics of the carbon atom allows to build molecules for which their mirror image is not superimposable with the original system. This characteristic is known as chirality. The importance of the chirality is manifested in the selection of a unique enantiomeric form for the two main building blocks of nature, the aminoacids and sugars.

Leaving aside the very small energy differences because of the parity violation principle,¹ that have never been measured for any organic molecule so far, both enantiomers present the same physicochemical properties in nonchiral environments. However, the effect of polarized light, which is chiral itself, can be used to distinguish the two different enantiomers or to favor a given reaction as has been shown in the case of molecular machines proposed by Feringa where the chirality of the systems is used to govern the cycle.²

Chiral recognition in complexes linked by hydrogen bonds has been studied experimentally³ and theoretically.⁴ In some cases, chiral systems can aggregate and form long chains or helix-shaped structures.^{5–8} The subsequent chemical processes along the chains can invert stepwise the chirality of the molecules producing what we have called racemization waves.⁹ The control and rationalization of these processes is of the utmost importance in the development of novel molecules designed as switches.¹⁰

Enantiomerically pure diaziridines, generally N,N'-disubstituted, were described by Mannschreck and Seitz in 1967^{11–16} and have been the object of continuous interest (for a review and a recent paper see refs 17, 18). In the solid state, the X-ray structure of only two N,N'-unsubstituted diaziridines has been described with CSD¹⁹ refcodes: OCIWUS and RAJQID. The first one contains at positions 3 a spiro chiral glucose residue,²⁰ while the second one has an achiral 3,3-pentamethylene substituent.²¹ In both cases, the NH protons are in a trans disposition and the hydrogen-bond network involves N–H···N bonds

forming chains in the case of OCIWUS²⁰ and more complex patterns in the case of RAJQID.²¹

In the present article, the chiral discrimination in diaziridine clusters, connected through hydrogen bonds (HBs), has been studied using density functional theory (DFT) methods. Clusters up to eight monomers have been considered. Different topologies of the clusters have been explored. The protonation and the subsequent proton transfer along the molecular chains have been studied. The evolution of the optical rotatory power has been explored in function of the cluster size.

Methods

The geometry of the isolated monomers, clusters, and transition-state structures has been optimized using the hybrid DFT, B3LYP computational level,^{22,23} and the 6-31+G** basis set,²⁴ with the Gaussian-03 package.²⁵ The minimum or transition state (TS) nature of the geometries has been verified by frequency calculations at the same computational level.

This computational level has been proven to be adequate for the description of hydrogen-bonded system providing similar results to the ones obtained at the MP2 level with a triple-Z basis set.^{26,27} Some calculations have been carried out at MP2 level to confirm this assertion.

ORP has been calculated at the B3LYP/6-311++G(2d,2p) level. This level of calculation has been considered as the minimum adequate to obtain reliable results.^{28–30}

We have not considered quantum tunneling in our study either of the inversion barriers or of the proton transfer. In what concerns inversion barriers, microwave studies on the H₂C=NH inversion show that tunneling adds little to the measured rates.³¹ Another degenerate system is found in the inversion of aziridine where the tunneling at 338–373 K has been estimated to 5% of ΔG^\ddagger .³² The tunneling is important at temperatures at which vibrational levels within 20–25 kJ mol⁻¹ of the top of the potential barrier are substantially populated.³³ In what concerns proton transfer, the effect of tunneling should be more important taking into account literature results for the case NH₄⁺···NH₃,^{34,35} the treatment of these effects both classically

* Author to whom correspondence should be addressed. Fax: 34 91 564 48 53. E-mail: ibon@iqm.csic.es.

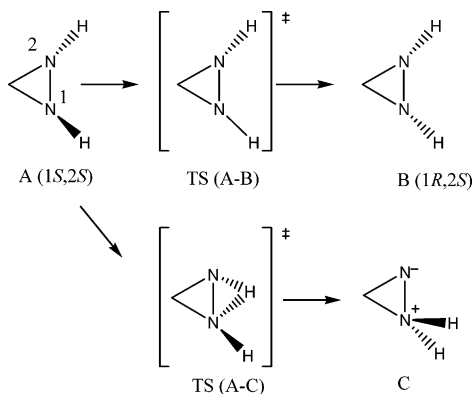


Figure 1. Schematic representation of the three possible tautomers of diaziridine and the TS linking them. The chirality of the stereogenic centers is indicated.

TABLE 1: Relative Energy of the Tautomers and TS Shown in Figure 1 Calculated at the B3LYP/6-31+G Computational Level**

structure	symmetry	B3LYP/6-31+G** E_{rel} (kJ mol ⁻¹)	MP2/6-31+G** E_{rel} (kJ mol ⁻¹)	MP2/6-311++G** E_{rel} (kJ mol ⁻¹)
A	C ₂	0.0	0.0	0.0
B	C _s	26.5	27.5	25.1
C	C _s	135.4	150.2	150.7
TS (A-B)	C ₁	119.0	133.5	149.6
TS (A-C)	C ₁	215.3	230.1	225.2

(using the Bell–Limbach model)^{36,37} and quantum mechanically^{38–40} is beyond the aims of the present work. However, we feel that in the examples reported in this paper the neglecting of the quantum mechanical tunneling should not alter the main conclusions.

Results and Discussion

Neutral Monomers. Initially, the three possible tautomers of diaziridine, A, B, and C, have been considered, together with the transition states between the most stable configuration A [(1*S*,2*S*)diaziridine] and the other two structures B [(1*R*,2*S*)diaziridine], which is a meso form, and C (Figure 1 and Table 1). The *SS* and *RR* nomenclature will be used along the text to refer to the (1*S*,2*S*)diaziridine and (1*R*,2*R*)diaziridine molecules, respectively.

The problem of the structure and inversion of diaziridines has been the subject of many studies, experimental^{18,41} as well as theoretical.^{42–45} If we have carried out the calculations corresponding to Figure 1 and Table 1, it is to have a set of

values consistent with those of the clusters and not to try to discuss previous work which was carried out at higher levels [MP4, G2, G3, CCSD(T)].^{42–45} However, the values of Table 1 are very similar to those reported in these studies, for instance, structure C calculated at the B3LYP/6-31+G** level (135.4 kJ mol⁻¹) is similar to the G2 calculation (135.6 kJ mol⁻¹) and at the MP2/6-311++G** level (150.7 kJ mol⁻¹) to the MP4/6-311G** level (150.2 kJ mol⁻¹).⁴³ The synchronous inversion of both nitrogens via a C_{2v} structure presents two imaginary frequencies, in agreement with previous reports,⁴⁴ and its relative energy is 264.2, 294.4, and 291.5 kJ mol⁻¹ at the three levels reported in Table 1.

The results obtained for the different methods and basis sets are qualitatively similar, even though the B3LYP method provides transition-state barriers 10% lower in average than those obtained at the MP2 level with the same basis set. The energy differences between the minima indicate that in the case of the isolated molecule, the most stable configuration corresponds to a chiral molecule, A or its enantiomer, while the meso form B is 26 kJ mol⁻¹ higher in energy and the zwitterionic one, C, is highly destabilized by 135 kJ mol⁻¹ at the B3LYP level. In addition, the energy barriers to transform configuration A into B or C are high in the gas phase. Structures B and C are intermediates in the racemization process of this molecule, since they can evolve to either A or its enantiomer A*.

Neutral Clusters. Five different topologies of the cluster that present two HB interactions per monomer have been considered (Figure 2 shows the optimized ones for the hexamer). The first three cases correspond to two homochiral (I and II in Figure 2) and one alternating chiral complexes (III). In those cases where the number of monomers is large enough, the homochiral complex can be present in helical and cyclic form in analogy to the experimental data of the HB clusters formed by systems with C₂ symmetry^{5,6} and in agreement with the theoretical recent reports of clusters of chiral molecules with the same symmetry.^{8,9,46} In addition, two clusters of monomer B with different topology have been considered (IV and V), those that can be considered as analogous to both the homo- and heterochiral cases and as will be seen later can be important in the proton-transfer mechanism. The relative energy results obtained at the MP2/6-31+G(d,p) computational level for the dimers and trimers are similar to those obtained at the B3LYP/6-31+G(d,p) one (Table 2).

The relative energies with respect to the noncyclic homochiral cluster (I) are shown in Figure 3. In all clusters, the most stable configuration corresponds to that with the alternated chirality. The cyclic homochiral clusters (II) present two more HBs than

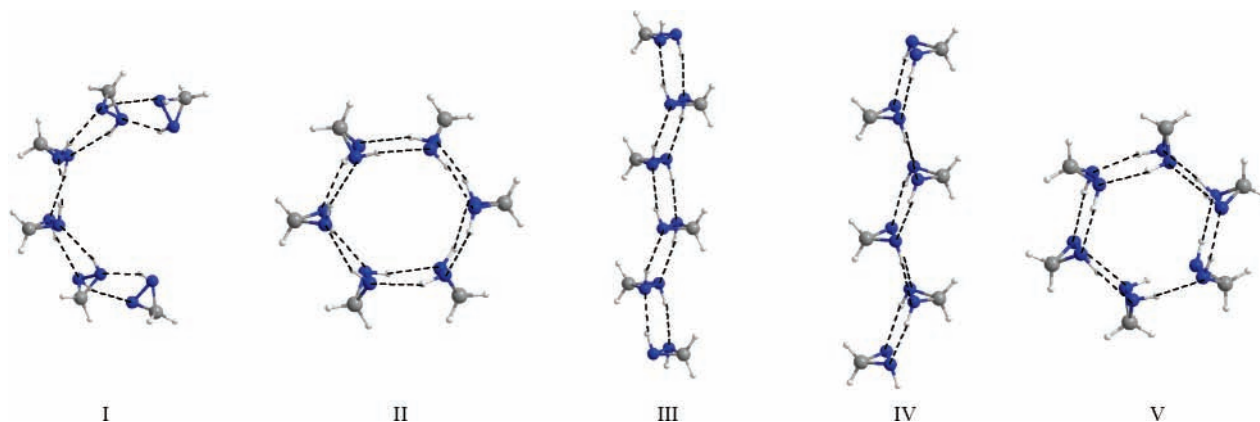


Figure 2. Optimized geometries of the five configurations considered for the clusters. The ones shown correspond to the hexamer. The identifiers I–V are used for all the cluster sizes studied.

TABLE 2: Relative Energy (kJ mol⁻¹) of the Different Configurations Considered for the Dimers and Trimers Calculated at the B3LYP/6-31+G and MP2/6-31+G** Computational Levels**

configuration	dimers		trimers	
	B3LYP/ 6-31+G**	MP2/ 6-31+G**	B3LYP/ 6-31+G**	MP2/ 6-31+G**
I	0.00	0.00	0.00	0.00
III	-2.83	-2.64	-5.28	-4.86
IV	49.59	52.05	66.16	71.07
V	50.96	55.05	43.37	37.19

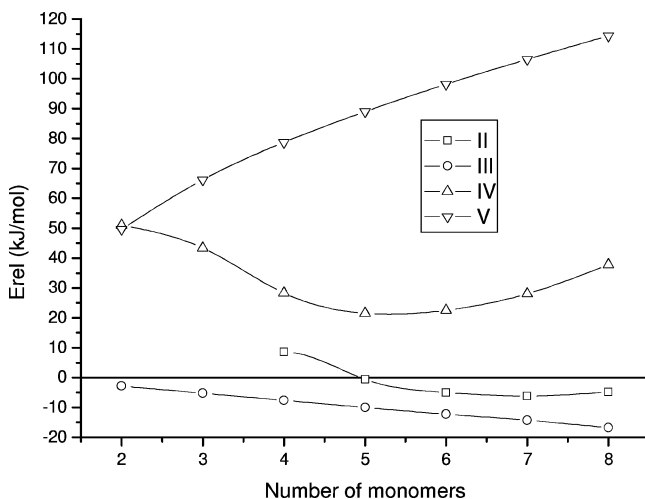
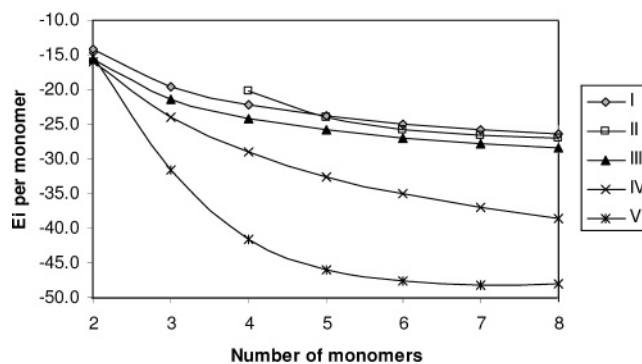
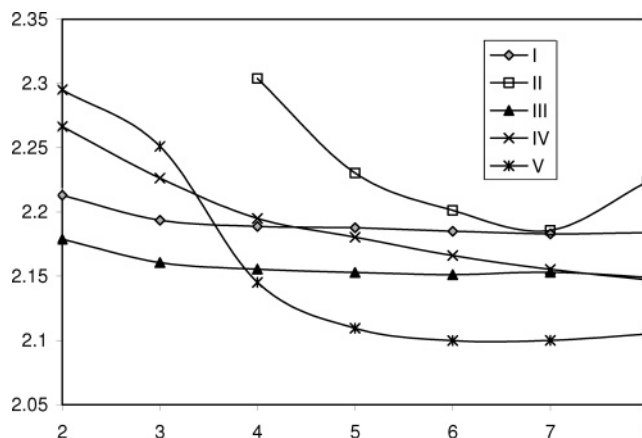
TABLE 3: Interaction Energy (kJ mol⁻¹) of the Clusters Studied with Respect to the Energy of the Former Monomers

cluster size	I	II	III	IV	V
2	-28.48		-31.31	-31.80	-30.43
3	-58.65		-63.94	-71.86	-94.65
4	-88.99	-80.46	-96.66	-116.09	-166.55
5	-119.40	-120.02	-129.47	-162.65	-230.19
6	-149.89	-154.92	-162.14	-210.44	-286.08
7	-180.38	-186.55	-194.68	-259.04	-337.48
8	-210.85	-215.73	-227.67	-308.12	-384.74

the noncyclic clusters (I) and are more stable than the noncyclic homochiral cluster for $n > 5$, being the most favorable case for the seven-membered complex with a E_{rel} of -6.14 kJ mol⁻¹ with respect to the noncyclic homochiral case and 8.13 kJ mol⁻¹ less stable than the case with alternated chirality (III).

The average interaction energy per monomer of the clusters studied is gathered in Table 3. In general, the interaction energy of clusters formed by meso forms, IV and V, presents larger interaction energies than those formed by the chiral monomers probably because of a favorable secondary HB interaction in the former cases^{47,48} and a most effective dipole-dipole interaction between the monomers. The structures with cyclic clusters, II and V, present their maximum energetic differences with respect to the noncyclic counterparts, I and IV, in the clusters with seven monomers. Thus, it can be assumed that this configuration is the most favorable for the cyclic configurations.

The energetic cooperativity of the clusters is evident when the interaction energy is plotted versus the number of monomers (Figure 4). Only the cyclic cluster V presents a minimum as an indication that the most favorable interaction energy per monomer has been reached and larger clusters should have smaller interaction energy per monomer. In the lineal cases,

**Figure 3.** Evolution of the relative energy, with respect to the noncyclic homochiral clusters (I), with the number of monomers.**Figure 4.** Interaction energy per monomer (kJ mol⁻¹) versus the number of monomers.**Figure 5.** Evolution of the average HB distance as a function of the number of monomers within the cluster.

the cluster size is not large enough to estimate the maximum interaction energy value that can be reached in very large clusters. In addition, the different behavior of the IV cluster with a deeper tendency is significant. These results can be related to the dipole moment component of each molecule in the direction of the hydrogen bonds. While the chiral molecule shows a small component in the direction of the HB, a much bigger one is expected in the meso forms. A similar result has been recently described for 4-pyridone clusters in linear HB arrangement where very large cooperativity effects have been found.⁴⁹

The energetic difference between the homochiral (I) and alternated cluster (III) is linearly related to the number of monomers ($R^2 = 0.999$) favoring the latter. Thus, in a long chain, as the ones encountered in solid phase, the alternated cluster should be energetically favored.

The evolution of the average HB distance as a function of the cluster size is shown in Figure 5. Small variations are observed in the noncyclic homochiral and heterochiral clusters (I and III, respectively). The two cyclic configurations, II and V, present a minimum value in the heptamer. Finally, configuration IV is the only one where the average distance tends to shorter values for clusters larger than eight monomers. This result is probably related to the effective alignment of the monomer dipole moment and compares well with the evolution of the interaction energy per monomer for the same configuration.

Proton Transfer in Neutral Systems. The proton transfer in the neutral and protonated systems along the chain has been studied for the monomers, dimer, and trimer isolated and in the presence of one and two water molecules, as solvent, at both ends of the chains. The proton transfer along the chain

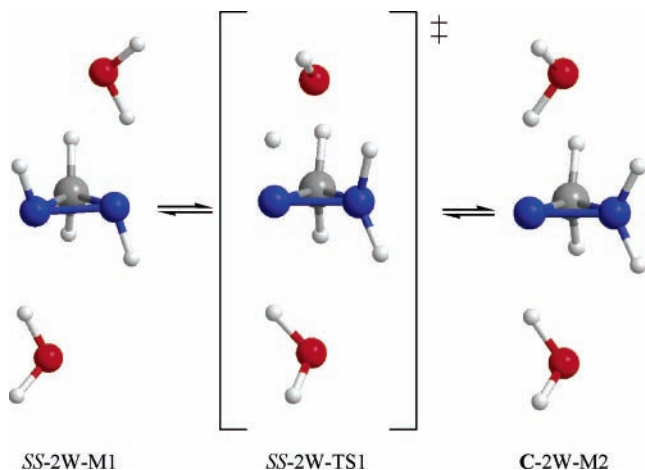


Figure 6. Minima and transition-state structures found in the proton transfer of the monomers in the presence of two water molecules (because of symmetry reasons, only half of the structures are shown). The TS structure has been named using the chirality of the precedent system in the figure.

TABLE 4: Relative Energy (kJ mol^{-1}) of the Proton-Transfer Stationary Structures within the Monomers in the Presence of Two and Four Water Molecules (See Figure 6)

number of water molecules	M1	TS	M2
2	0.00	134.84	91.99
4	0.00	89.88	66.01

produces the racemization of the monomers that have been involved in this process. Once the proton reaches the last monomer of the chain, it has two possibilities, go back to the original configuration or produce the racemization of the chain if it evolves using the other N atom of each diaziridine molecule. This process is similar to the Grotthuss mechanism,⁵⁰ where the entering proton does not leave the chain until n other protons enter, where n is the number of hydrogen bonds in the chain. Another mechanism where the presence of HB is not necessary has been described recently but does not apply to the present case.⁵¹

The results obtained for the proton transfer within the monomer in the presence of two water molecules are shown in Figure 6 and Table 4. The comparison of the proton-transfer TS without the water molecules (see Table 1) shows that the presence of solvent molecules stabilizes 80 kJ mol^{-1} the TS

TABLE 5: Relative Energy, with Respect to the Energy of the Corresponding M1 Structure, and Chiral Discrimination (kJ mol^{-1}) in the Stationary Structures along the Proton-Transfer Path in the Homo- and Heterochiral Dimers (See Figure 7)

starting structure	M1	TS1	M2	TS2
SS:SS	0.00	200.03	110.29	179.65
RR:SS	0.00	205.52	109.96	167.71
chiral discr.	-2.83	2.66	-3.15	-11.93
SS:SS-2W ^a	0.00	129.49	89.64	154.26
RR:SS-2W	0.00	128.67	89.04	146.29
chiral discr.	-2.51	-3.33	-3.11	-10.48
SS:SS-4W ^a	0.00	92.19	75.30	139.79
RR:SS-4W	0.00	91.34	74.79	132.61
chiral discr.	-2.58	-3.43	-3.09	-9.77

^a 2W and 4W indicate the presence of two and four molecules of water.

structure, for the first two ones, and 45 kJ mol^{-1} for the two additional water molecules. In addition, the zwitterion structure M2 is stabilized by 42 kJ mol^{-1} and 26 kJ mol^{-1} because of the presence of two and four water molecules, respectively, since it forms stronger HB contacts than the parent compound.

The results of the proton transfer within the neutral homo-chiral and heterochiral dimers without and with two and four molecules of water are shown in Figure 7 and Table 5. In the absence of water molecules, a reduction of 10 kJ mol^{-1} is observed in the intramolecular proton transfer with respect to that of the isolated monomer, which corresponds to the limiting step in this reaction. The intermediate formed by a nonchiral and a chiral structure is stabilized over 25 kJ mol^{-1} when compared to the relative energy of the isolated nonchiral because of the formation of strong HB as occurs in the solvated monomer. The inclusion of solvent molecules produces a significant reduction of the first proton transfer (TS1), over 70 kJ mol^{-1} with two water molecules and about 109 kJ mol^{-1} with four molecules, and thus the limiting step becomes the intermolecular proton transfer (TS2), even though it is stabilized between 21 and 40 kJ mol^{-1} because of the presence of the external water molecules. The intermediate structure (M2) with a nonchiral molecule is again stabilized over 20 kJ mol^{-1} with respect to the system without solvent molecules.

The results of the proton transfer for the trimers without and with water molecules (Figure 8 and Table 6) are very similar to the ones reported for the dimers as an indication that these

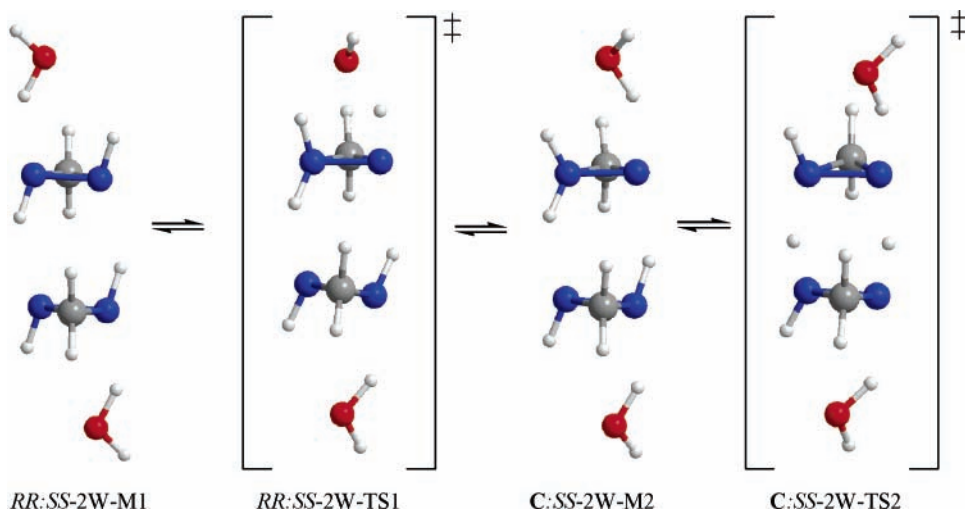


Figure 7. Minima and transition-state structures found in the proton transfer of the heterochiral dimer in the presence of two water molecules (because of symmetry reasons, only half of the structures are shown). The TS structures have been named using the chirality of the precedent system in the figure.

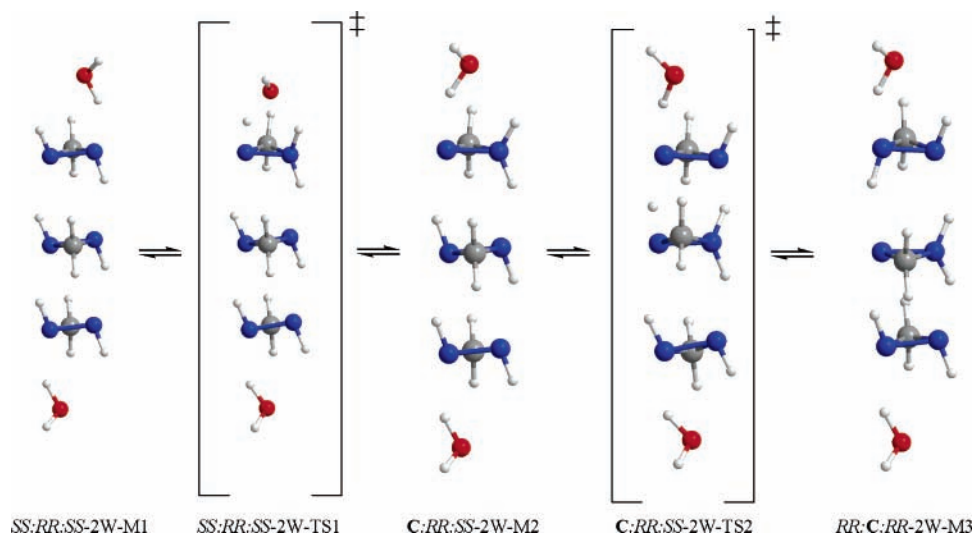


Figure 8. Minima and transition-state structures found in the proton transfer of the trimer with alternated chirality in the presence of two water molecules (because of symmetry reasons, only half of the structures are shown). The TS structures have been named using the chirality of the precedent system in the figure.

TABLE 6: Relative Energy and Chiral Discrimination (kJ mol⁻¹) in the Stationary Structures along the Proton-Transfer Path in the Homo- and Alternated Chiral Trimers (See Figure 8)

	M1	TS1	M2	TS2	M3
SS:SS:SS	0.00	201.47	107.67	166.28	91.36
SS:RR:SS	0.00	201.98	107.94	158.31	90.39
chiral discr.	-5.28	-4.78	-5.01	-13.25	-6.25
SS:SS:SS-2W	0.00	127.77	88.56	147.37	87.64
SS:RR:SS-2W	0.00	127.59	88.86	139.66	87.25
chiral discr.	-5.38	-5.56	-5.08	-13.09	-5.77
SS:SS:SS-4W	0.00	91.61	75.99	141.67	84.90
SS:RR:SS-4W	0.00	91.16	75.52	134.37	84.51
chiral discr.	-5.00	-5.45	-5.47	-12.30	-5.40

chains are adequate models for larger cases. The proton transfer along the chain produces an inversion of the chirality of the monomers as can be seen clearly in the first and last structures shown in Figure 8. This effect should invert the chirality of the monomers in longer chains as the proton transfer evolves along the chain producing what has been named as chirality wave.

Regarding the chiral discrimination observed for the different species in the proton-transfer process, a significant increment of its value is obtained in the TS2 structures of the dimers and trimers, which corresponds to the intermolecular proton transfer. These results can be explained on the basis of the contraction of the systems upon proton transfer that increases the repulsion of the CH₂ group of the diaziridine molecules in the homochiral complexes.^{27,52}

Protonated Systems. The protonation of the monomer does not destroy the chirality of this molecule. However, now only one stereogenic center is present in the molecule and the proton transfer, from one nitrogen to the other one, or the inversion of the NH group produces the racemization of the system (Figure 9). The barrier of this process will be discussed.

In the dimers and larger clusters, the protonation in the external molecules of the noncyclic homo- and heterochiral clusters spontaneously produces a proton transfer to the second molecule of the chain. A similar process has been described for the protonation process of HCN and formamide clusters^{53,54} and protein α -helix models.⁵⁵ The basicity of the systems (Table 7) increases with the size of the cluster because of the solvation effect of the additional monomers (similar effects have been

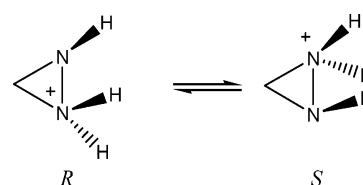


Figure 9. Schematic representation of the protonated diaziridine. The chirality of the stereogenic nitrogen is shown.

TABLE 7: Proton Affinity with Respect to the Corresponding Neutral Complex

	PA (kJ mol ⁻¹)	chiral discrimination protonated
SS	-884.12	
SS:SS	-965.93	
RR:SS	-966.19	-3.08
(SS) ₃	-1008.84	
SS:RR:SS	-1007.00	-3.44
(SS) ₄	-1022.73	
(RR:SS) ₂	-1018.65	-3.59

described for HB clusters of water). This process generates a mesolike structure in the first member of the chain (Figure 10).

In the protonated chains, the proton transfer produces, in a first step, the formation of mesoforms of diaziridine along the chain. Thus, if the proton leaves at the end of the chain, the configurations IV and V are obtained from the initial II and III forms, respectively.

Protonation produces important geometrical variation on the direction of the chains with a kink in the second monomer, which is the one that becomes protonated. This molecule acts, mainly, as HB donor, forming a short NH \cdots N with the third molecule while the HB where the second molecule acts as acceptor is elongated over 3 Å in the trimers and tetramers studied here.

As in the neutral systems, the configuration with alternated chirality is more stable than the homochiral one. However, in this case, the increment of the difference between these two configurations with the cluster size is not as pronounced as in the neutral clusters (the energetic difference between the neutral configurations I and III are -2.83, -5.29, and -7.67 kJ mol⁻¹ for the dimer, trimer, and tetramer, respectively).

The proton transfer in these systems has been studied without and with one molecule of water at the end of the chain (Table

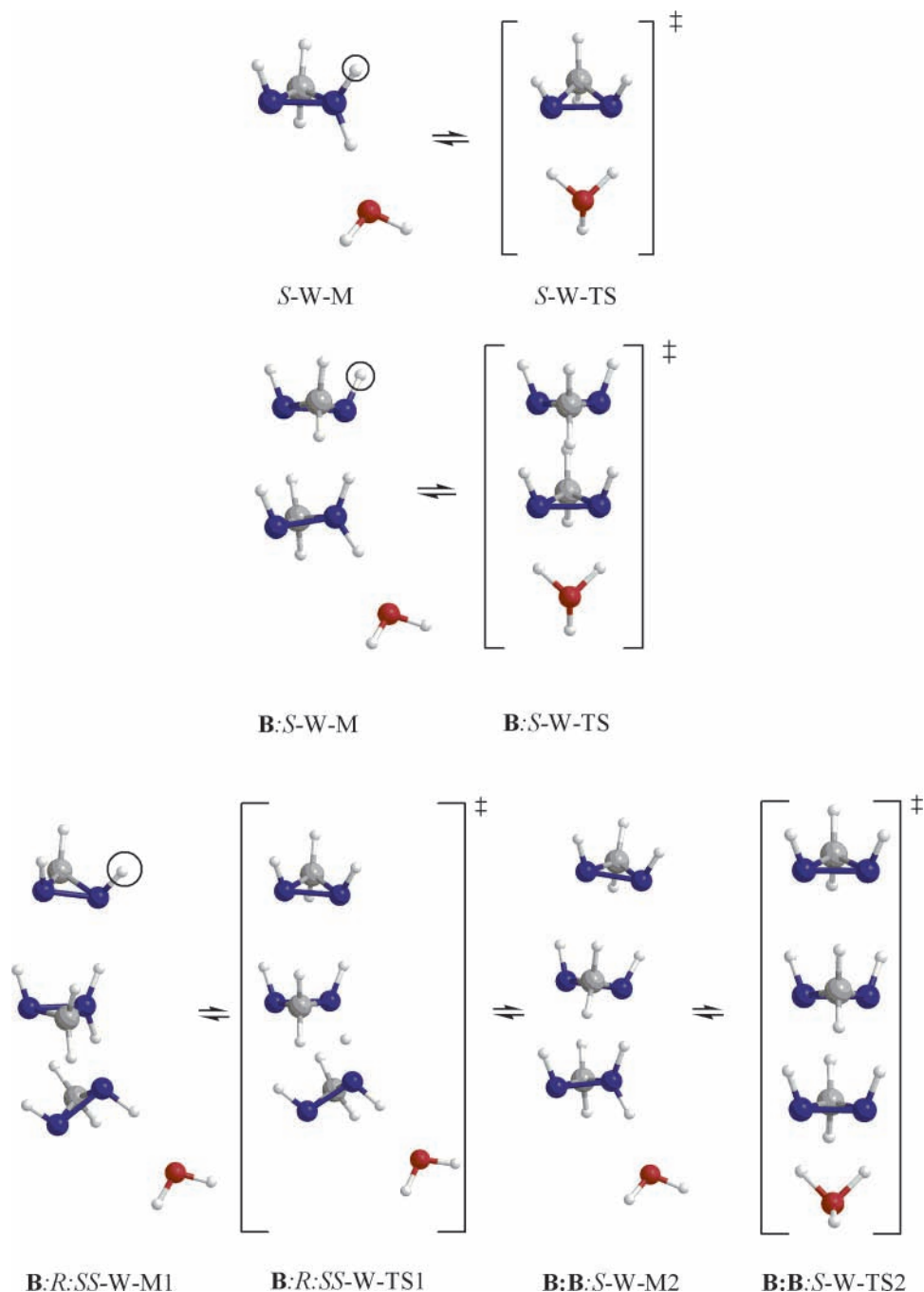


Figure 10. Proton-transfer process in the presence of a water molecule for the monomer, heterochiral dimer, and trimer with alternating chirality as starting structures (because of symmetry reasons, only half of the structures are shown). The circle hydrogen atom corresponds to the proton added to the molecules. The TS structures have been named using the chirality of the precedent system in the figure.

8 and Figure 10). The process evolves with a smaller barrier than in the case of the neutral ones. In all the cases, the limiting step is the intramolecular proton transfer at the end of the chain. However, the presence of more solvent molecules should reduce it, and thus in the case of the monomer the proton transfer with two molecules of water in the molecular side where the reaction takes place provides a barrier of only 33 kJ mol^{-1} .

As the proton advances along the chain, the molecules lose their chirality and thus when the proton reaches the last monomer, only that one has chirality. If the proton is released at the end of the chain, the whole chain becomes nonchiral but energetically less stable than the original one, as shown in the study of the neutral clusters.

Optical Rotatory Power (ORP). The calculated ORP of the homochiral linear and cyclic clusters I and II are gathered in

Table 9. The values obtained here are similar to the ones reported for the diaziridine molecule calculated with the aug-cc-pVDZ and 6-311+ +G(2d,2p) basis sets 67.7 and 62.1° , respectively.⁵⁶ The shape of the cluster has a deep influence on the value and sign of the ORP. Thus, while the monomer and cyclic structures have positive values of ORP, the structure I that has a helix shape presents in all the cases negative values.

In the case of the cyclic clusters, II, a linear correlation can be found between the ORP value and the number of monomers of the cluster ($\text{ORP} = 11.7 (n^\circ \text{ of monomers}) + 17.31$, $R^2 = 0.99$, $n = 5$).

The protonation of the monomer does not change significantly the ORP of this molecule. However, in the dimer, trimer, and

TABLE 8: Energetics (kJ mol⁻¹) of the Proton-Transfer Processes in the Protonated Monomer, Dimers, and Trimers

starting geometries	M	TS		
SS	0.00	179.02		
SS-W	0.00	82.55		
SS-2W ^a	0.00	32.76		
	M	TS		
SS:SS	0.00	174.67		
RR:SS	0.00	175.49		
chiral discr.	-3.08	-2.26		
SS:SS-W	0.00	98.96		
RR:SS-W	0.00	99.32		
chiral discr.	-2.81	-2.44		
	M1	TS1	M2	TS2
SS:SS:SS	0.00	<i>b</i>	14.71	189.22
SS:RR:SS	0.00	<i>b</i>	13.54	188.62
chiral discr.	-3.44		-4.62	-4.04
SS:SS:SS-W	0.00	3.45	-3.97	100.76
SS:RR:SS-W	0.00	2.72	-5.13	98.90
chiral discr.	-3.59	-4.33	-4.75	-5.45

^a In this case the two water molecules are in the same side of the aziridine molecule. ^b The corresponding TS1 without solvent molecules have not been located.

TABLE 9: Frequency Independent and Dependent ORP (°) of the Linear and Cyclic Homochiral Clusters

	configuration I		configuration II	
	$\alpha_{D(0)}$	α_D	$\alpha_{D(0)}$	α_D
SS	44.61	58.79		
(SS) ₂	-132.12	-138.84		
(SS) ₃	-204.00	-219.59		
(SS) ₄	-231.16	-249.16	57.61	64.15
(SS) ₅	-262.13	-284.04	63.57	74.3
(SS) ₆	-290.79	-316.64	73.41	88.64
(SS) ₇	-311.10	-339.74	81.41	101.62
(SS) ₈	-328.60	-359.55	84.96	109.02
SS(H ⁺)	36.82	42.41		
(SS) ₂ (H ⁺)	-31.48	-35.49		
(SS) ₃ (H ⁺)	-28.58	-32.52		
(SS) ₄ (H ⁺)	-74.35	-81.00		

tetramer, the value is reduced even though it still has the opposite sign of the monomer as in the case of the neutral clusters.

Conclusions

A study of the chiral discrimination in diaziridine clusters has been carried out using DFT computational methods. The most stable neutral structure corresponds to that with the monomers in alternated chirality. The proton transfer within the neutral diaziridine chain proceeds with high TS barriers. The protonation of the first diaziridine of the chain tends to produce a spontaneous proton transfer from the first monomer to the second. The studied processes of proton transfer in the charged system show small barriers. The proton transfer in the neutral or protonated systems produces an inversion of the chirality of the monomers as the process evolves along the chain producing chirality waves. The calculated ORP of the clusters is very dependent on the cluster size, cyclic or helix shape, and the number of monomers that form the cluster.

Although diaziridine itself has not been prepared, many 3-substituted and 3,3'-disubstituted diaziridine derivatives are known. Therefore, experiments verifying the theoretical findings

in the present paper may either be carried out in solution or else by gas-phase spectroscopy. The issue of alternating chirality cluster preferences has recently been experimentally verified in the case of lactate tetramers; however, in that case, the chirality is more permanent.⁵⁷ A case of chirality synchronization in transiently chiral cluster species has been recently published for trifluoroethanol.⁵⁸

Acknowledgment. This work was carried out with financial support from the Ministerio de Educación y Ciencia (Project No. BQU2003-01251 and CTQ2006-14487-C02-01/BQU) and Comunidad Autónoma de Madrid (Project MADRISOLAR, ref S-0505/PPQ/0225). Thanks are given to the CTI (CSIC) and CESA for allocation of computer time. K. Z. acknowledges the grant given by Ministerio de Educación y Ciencia of Spain (SB2004-0010).

References and Notes

- Quack, M. *Angew. Chem., Int. Ed. Engl.* **1989**, *28*, 571.
- Feringa, B. L. *Science* **2001**, *292*, 2021.
- Speranza, M.; Satta, M.; Piccirillo, S.; Rondino, F.; Paladini, A.; Giardini, A.; Filippi, A.; Catone, D. *Mass Spectrom. Rev.* **2005**, *24*, 588.
- Alkorta, L.; Picazo, O.; Elguero, J. *Curr. Org. Chem.* **2006**, *10*, 695.
- Stoncius, S.; Orentas, E.; Butkus, E.; Ohrstrom, L.; Wendt, O. F.; Warnmark, K. *J. Am. Chem. Soc.* **2006**, *128*, 8272.
- Brienne, M. J.; Gabard, J.; Leclercq, M.; Lehn, J. M.; Cesario, M.; Pascard, C.; Cheve, M.; Dutrucrosset, G. *Tetrahedron Lett.* **1994**, *35*, 8157.
- Alkorta, I.; Zborowski, K.; Elguero, J. *Chem. Phys. Lett.* **2006**, *427*, 289.
- Elango, M.; Parthasarathi, R.; Subramanian, V.; Ramachandran, C. N.; Sathyamurthy, N. *J. Phys. Chem. A* **2006**, *110*, 6294.
- Alkorta, I.; Picazo, O.; Elguero, J. *J. Phys. Chem. A* **2006**, *110*, 2259.
- Feringa, B. L. *Molecular Switches*; Wiley-VCH: Weinheim, Germany, 2001.
- Mannsch, A.; Radeaglia, R.; Grundema, E.; Ohme, R. *Chem. Ber./Recl.* **1967**, *100*, 1778.
- Mannsch, A.; Seitz, W. *Angew. Chem., Int. Ed. Engl.* **1969**, *8*, 212.
- Haselbac, E.; Mannsch, A.; Seitz, W. *Helv. Chim. Acta* **1973**, *56*, 1614.
- Hakli, H.; Mannschreck, A. *Angew. Chem., Int. Ed. Engl.* **1977**, *16*, 405.
- Hakli, H.; Mintas, M.; Mannschreck, A. *Chem. Ber./Recl.* **1979**, *112*, 2028.
- Mintas, M.; Mannschreck, A.; Klasinc, L. *Tetrahedron* **1981**, *37*, 867.
- Kostyanovsky, R. G.; Murugan, R.; Sutharchanadevi, M. *Comprehensive Heterocyclic Chemistry II*; Pergamon: Oxford, U.K., 1996; Vol. 1A.
- Trapp, O.; Schurig, V.; Kostyanovsky, R. G. *Chem.—Eur. J.* **2004**, *10*, 951.
- Allen, F. H. *Acta Crystallogr., Sect. B* **2002**, *58*, 380.
- Bluchel, C.; Linden, A.; Vasella, A. *Helv. Chim. Acta* **2001**, *84*, 3495.
- Charette, A. B.; Legault, C.; Belanger-Gariepy, F. *Acta Crystallogr., E* **2004**, *60*, O1921.
- Becke, A. D. *J. Chem. Phys.* **1993**, *98*, 5648.
- Lee, C. T.; Yang, W. T.; Parr, R. G. *Phys. Rev. B* **1988**, *37*, 785.
- Hariharan, P. C.; Pople, J. A. *Theor. Chim. Acta* **1973**, *28*, 213.
- Frisch, M. J.; Trucks, G. W.; Schlegel, H. B.; Scuseria, G. E.; Robb, M. A.; Cheeseman, J. R.; Montgomery, J. A., Jr.; Vreven, T.; Kudin, K. N.; Burant, J. C.; Millam, J. M.; Iyengar, S. S.; Tomasi, J.; Barone, V.; Mennucci, B.; Cossi, M.; Scalmani, G.; Rega, N.; Petersson, G. A.; Nakatsuji, H.; Hada, M.; Ehara, M.; Toyota, K.; Fukuda, R.; Hasegawa, J.; Ishida, M.; Nakajima, T.; Honda, Y.; Kitao, O.; Nakai, H.; Klene, M.; Li, X.; Knox, J. E.; Hratchian, H. P.; Cross, J. B.; Bakken, V.; Adamo, C.; Jaramillo, J.; Gomperts, R.; Stratmann, R. E.; Yazyev, O.; Austin, A. J.; Cammi, R.; Pomelli, C.; Ochterski, J. W.; Ayala, P. Y.; Morokuma, K.; Voth, G. A.; Salvador, P.; Dannenberg, J. J.; Zakrzewski, V. G.; Dapprich, S.; Daniels, A. D.; Strain, M. C.; Farkas, O.; Malick, D. K.; Rabuck, A. D.; Raghavachari, K.; Foresman, J. B.; Ortiz, J. V.; Cui, Q.; Li, A. G.; Clifford, S.; Cioslowski, J.; Stefanov, B. B.; Liu, G.; Liashenko, A.; Piskorz, P.; Komaromi, I.; Martin, R. L.; Fox, D. J.; Keith, T.; Al-Laham, M. A.; Peng, C. Y.; Nanayakkara, A.; Challacombe, M.; Gill, P. M. W.; Johnson, B.; Chen, W.; Wong, M. W.; Gonzalez, C.; Pople, J. A. *Gaussian-03*, Gaussian-03 ed.; Gaussian, Inc.: Wallingford, CT, 2003.

- (26) Alkorta, I.; Elguero, J. *J. Chem. Phys.* **2002**, *117*, 6463.
- (27) Picazo, O.; Alkorta, I.; Elguero, J. *J. Org. Chem.* **2003**, *68*, 7485.
- (28) Cheeseman, J. R.; Frisch, M. J.; Devlin, F. J.; Stephens, P. J. *J. Phys. Chem. A* **2000**, *104*, 1039.
- (29) Stephens, P. J.; Devlin, F. J.; Cheeseman, J. R.; Frisch, M. J. *J. Phys. Chem. A* **2001**, *105*, 5356.
- (30) Ruud, K.; Stephens, P. J.; Devlin, F. J.; Taylor, P. R.; Cheeseman, J. R.; Frisch, M. J. *Chem. Phys. Lett.* **2003**, *373*, 606.
- (31) Kemp, M. K.; Flygare, W. H. *J. Am. Chem. Soc.* **1968**, *90*, 6267.
- (32) Carter, R. E.; Drakenberg, T.; Bergman, N. A. *J. Am. Chem. Soc.* **1975**, *97*, 6990.
- (33) Rauk, A.; Allen, L. C.; Mislow, K. *Angew. Chem., Int. Ed. Engl.* **1970**, *9*, 400.
- (34) Manca, C.; Tanner, C.; Coussan, S.; Bach, A.; Leutwyler, S. *J. Chem. Phys.* **2004**, *121*, 2578.
- (35) Rosso, L.; Tuckerman, M. E. *Pure Appl. Chem.* **2004**, *76*, 49.
- (36) Limbach, H. H.; Manz, J. *Ber. Bunsen. Phys. Chem.* **1998**, *102*, 289.
- (37) Klein, O.; Aguilar-Parrilla, F.; Lopez, J. M.; Jagerovic, N.; Elguero, J.; Limbach, H. H. *J. Am. Chem. Soc.* **2004**, *126*, 11718.
- (38) Shida, N.; Almlöf, J.; Barbara, P. F. *J. Phys. Chem.* **1991**, *95*, 10457.
- (39) Tautermann, C. S.; Voegelé, A. F.; Loerting, T.; Liedl, K. R. *J. Chem. Phys.* **2002**, *117*, 1962.
- (40) Xue, Q.; Horsewill, A. J.; Johnson, M. R.; Trommsdorff, H. P. *J. Chem. Phys.* **2004**, *120*, 11107.
- (41) Trapp, O. *Chirality* **2006**, *18*, 489.
- (42) Alcami, M.; Mo, O.; Yanez, M. *J. Comput. Chem.* **1998**, *19*, 1072.
- (43) Alcami, M.; Mo, O.; Yanez, M. *J. Mol. Struct.: THEOCHEM* **1998**, *433*, 217.
- (44) Nielsen, I. M. B. *J. Phys. Chem. A* **1998**, *102*, 3193.
- (45) Gessner, K. J.; Ball, D. W. *J. Mol. Struct.: THEOCHEM* **2005**, *130*, 95.
- (46) Alkorta, I.; Zborowski, K.; Elguero, J. *Chem. Phys. Lett.* **2006**, *427*, 289.
- (47) Jorgensen, W. L.; Pranata, J. *J. Am. Chem. Soc.* **1990**, *112*, 2008.
- (48) Alvarez-Rua, C.; Garcia-Granda, S.; Goswami, S.; Mukherjee, R.; Dey, S.; Claramunt, R. M.; Santa Maria, M. D.; Rozas, I.; Jagerovic, N.; Alkorta, I.; Elguero, J. *New J. Chem.* **2004**, *28*, 700.
- (49) Chen, Y. F.; Dannenberg, J. J. *J. Am. Chem. Soc.* **2006**, *128*, 8100.
- (50) Hertz, H. G.; Braun, B. M.; Müller, K. J.; Maurer, R. *J. Chem. Educ.* **1987**, *64*, 777.
- (51) Alkorta, I.; Elguero, J. *Org. Biomol. Chem.* **2006**, *4*, 3096.
- (52) Ramos, M.; Alkorta, I.; Elguero, J.; Golubev, N. S.; Denisov, G. S.; Benedict, H.; Limbach, H. H. *J. Phys. Chem. A* **1997**, *101*, 9791.
- (53) Sanchez, M.; Provasi, P. F.; Aucar, G. A.; Alkorta, I.; Elguero, J. *J. Phys. Chem. B* **2005**, *109*, 18189.
- (54) Moisan, S.; Dannenberg, J. J. *J. Phys. Chem. B* **2003**, *107*, 12842.
- (55) Wiczorek, R.; Dannenberg, J. J. *J. Am. Chem. Soc.* **2004**, *126*, 12278.
- (56) Qu, W. X.; Tabisz, G. C. *J. Chem. Phys.* **2006**, *124*, 184305.
- (57) Adler, T. B.; Borho, N.; Reiher, M.; Suhm, M. A. *Angew. Chem., Int. Ed.* **2006**, *45*, 3440.
- (58) Scharge, T.; Haber, T.; Suhm, M. A. *Phys. Chem. Chem. Phys.* **2006**, *8*, 4664.